High-Performance Supercapacitors Based on Poly(ionic liquid)-Modified Graphene Electrodes

Tae Young Kim,[†] Hyun Wook Lee,[†] Meryl Stoller,[‡] Daniel R. Dreyer,[§] Christopher W. Bielawski,[§] Rodney S. Ruoff,[‡,*] and Kwang S. Suh[†,*]

[†]Department of Materials Science and Engineering, Korea University, 5-1 Anam-dong Seongbuk-gu, Seoul 136-713, South Korea, [‡]Department of Mechanical Engineering and the Texas Materials Institute, The University of Texas at Austin, One University Station C2200, Austin, Texas 78712, United States, and [§]Department of Chemistry and Biochemistry, The University of Texas at Austin, One University Station A5300, Austin, Texas 78712, United States

ABSTRACT We report a high-performance supercapacitor incorporating a poly(ionic liquid)-modified reduced graphene oxide (PIL:RG-O) electrode and an ionic liquid (IL) electrolyte (specifically, 1-ethyl-3-methylimidazolium bis(trifluoromethylsulfonyl)amide or EMIM-NTf_2). PIL:RG-O provides enhanced compatibility with the IL electrolyte, thereby increasing the effective electrode surface area accessible to electrolyte ions. The supercapacitor assembled with PIL:RG-O electrode and EMIM-NTf_2 electrolyte showed a stable electrochemical response up to 3.5 V operating voltage and was capable of yielding a maximum energy density of 6.5 W · h/kg with a power density of 2.4 kW/kg. These results demonstrate the potential of the PIL:RG-O material as an electrode in high-performance supercapacitors.

KEYWORDS: supercapacitors · electrical double layers · graphene · ionic liquids · thermal reduction · ultracapacitors

Supercapacitors (also called electric double-layer capacitors or ultracapacitors) are electrochemical capacitors that store energy through reversible ion adsorption onto active materials that have high specific surface area.[1] Because of their many advantageous properties, such as high power density, high capacitance, and long cycle life (>100 000 cycles), these systems play an important role in electrical energy storage.[1−3] To generate a high specific capacitance, the specific surface area of the electrode materials needs to be as high as possible to accommodate a large number of electrolyte ions at the electrode/electrolyte interface thereby promoting the electrical double-layer capacitance.[1−3]

Graphene, an atom-thick 2D nanostructure,[4,5] is a promising material for supercapacitor electrodes owing to its low mass density, excellent electronic conductivity, and high surface area (~2630 m^2/g, theoretical).[6−8] Reduced graphene oxide (we use the generic term "RG-O"), a composition closely related to graphene, is a promising material for supercapacitor applications, as specific capacitance values of 135 and 99 F/g based on RG-O-based electrodes in aqueous and organic electrolytes, respectively, have been obtained.[6] However, dispersed graphene oxide (G-O) platelets can agglomerate during reduction by, for example, hydrazine in a solvent system such as water, resulting in the possible decrease of effective surface area, resulting in a lower specific capacitance than might be expected for an ideal graphene-based supercapacitor.[6] Moreover, current supercapacitors have energy densities well below the values required to provide power assists in various applications including hybrid electric vehicles or other high energy uses.[2,9] Hence, recent efforts have been focused on the development of supercapacitors with high energy densities, which may be achieved both by enhancing the operating voltage of the devices and by improving the accessibility of the ions from the electrolyte to the active regions of electrode materials.

Toward this goal, graphene-based electrodes combined with ionic liquid (IL) electrolytes can provide an attractive alternative for supercapacitors since such combinations result in an optimal pairing of high specific surface area electrodes and wider operating potentials that may be afforded by some IL electrolytes. Generally, ILs feature moderately high ion conductivity, nonvolatility, high decomposition temperatures, and wide electrochemical stability windows, and many ILs are being considered as electrolytes to increase supercapacitor operating voltages.[10−13] Despite the potential of ILs as electrolytes, further work is needed to explore their potential for supercapacitors assembled with graphene-based electrodes. One of the challenges is achieving graphene-based

*Address correspondence to suhkwang@korea.ac.kr, r.ruoff@mail.utexas.edu.

Received for review August 10, 2010 and accepted December 01, 2010.

Published online Xxxxxxxxx 00, 0000
10.1021/nn101968p

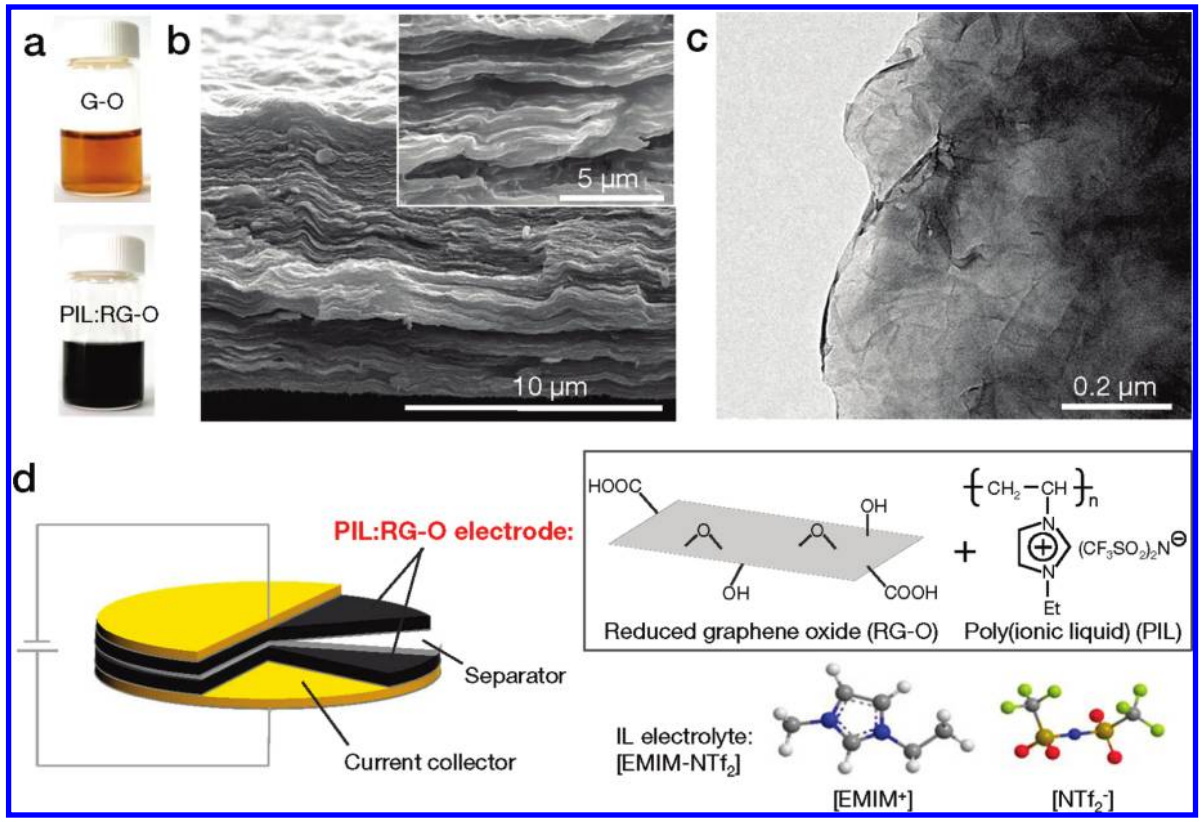

Figure 1. (a) Optical images of a suspension of a graphene oxide (G-O) in propylene carbonate (PC) and a poly(ionic liquid)-modified reduced graphene oxide (PIL:RG-O) in PC. (b) Scanning electron microscopy (SEM) and (c) transmission electron microscopy (TEM) image of PIL:RG-O platelets. (d) Schematic diagram of the supercapacitor based on the PIL:RG-O electrodes and ionic liquid electrolyte (EMIM-NTf_2).

electrode materials capable of being well wetted by the chosen ILs,[2,10] which may be attainable by the surface modification of graphene.

Herein, we report our progress toward high-performance supercapacitors based on poly(ionic liquid)-modified RG-O electrodes and an IL electrolyte, 1-ethyl-3-methylimidazolium bis(trifluoromethylsulfonyl)amide or EMIM-NTf_2. Poly(ionic liquid) (PIL) polymers formed from IL monomers can be prepared by the polymerization of unsaturated salts. Specifically, the use of poly(1-vinyl-3-ethylimidazolium) salts bearing the bis(trifluoromethylsulfonyl)amide anion (NTf_2^- or $CF_3SO_2-N-SO_2CF_3$) has been reported by our group to effectively stabilize hydrazine-reduced graphene oxide (RG-O) platelets *via* electrostatic and cation$-\pi$ interactions, resulting in the formation of PIL-modified RG-O materials.[14] The PIL-modified RG-O material (PIL:RG-O) can be produced simply by reduction in propylene carbonate (PC) at elevated temperature as recently reported,[15] where graphene oxide (G-O) platelets were suspended with the PIL in propylene carbonate and the suspension was thermally treated at ~150 °C[15] to yield PIL:RG-O (in PIL-modified RG-O material, the PIL is likely physisorbed to surface of RG-O platelet and not covalently linked). These *PIL-modified reduced G-O* materials (referred to here as PIL:RG-O) are expected to offer advantages for supercapacitor applications in that they should provide enhanced compatibility with certain IL electrolytes and improved accessibility of IL electrolyte ions into the graphene electrodes. Therefore, an additional aim of this paper was to illustrate the potential for using PIL:RG-O as an electrode material in supercapacitors incorporating IL electrolytes such as EMIM-NTf_2. Ultimately, a supercapacitor assembled with such a PIL:RG-O electrode and with EMIM-NTf_2 as the electrolyte exhibited (i) a specific capacitance of 187 F/g, (ii) an energy density of 6.5 W · h/kg, and (iii) a power density of 2.4 kW/kg.

The production of PIL:RG-O electrode materials was achieved through a thermal reduction of G-O suspension in propylene carbonate (PC)[15] containing PIL; the synthesis procedure is given in the Methods section. Briefly, 75 mg of PIL was dissolved in PC (20 mL) and 20 mg of graphite oxide (GO) powder was exfoliated and suspended by mild sonication in the PC/PIL mixture. Then, the suspension was heated at 150 °C for 1 h, which yielded a homogeneous black-colored suspension without any visible precipitation. The reduction of G-O platelets in PC in the presence of PIL at 150 °C occurred more readily than in a control experiment where no PIL was present,[15] as indicated by a lower surface resistivity value for a thin PIL:RG-O film (3 kΩ/sq) as compared to a thin film composed of overlapped and stacked reduced G-O platelets (505 kΩ/sq). The rapid re-

duction of suspended G-O platelets in PC with PIL by thermal treatment described here may provide a facile and economical processing route for such applications as electrode materials in supercapacitors, which had been previously suggested for suspensions of G-O platelets when heat treated in PC alone.[15] The PIL:RG-O electrode material was then recovered by vacuum filtration, and excess PIL was washed away with additional PC. The PIL:RG-O was composed of overlapped and stacked RG-O platelets that we believe were coated with PIL. The value of the zeta potential from the GO suspension in PC was −9.3 mV due to the negatively charged surface of the GO platelets. In contrast, the introduction of the PIL into the GO suspension in PC resulted in the reversal of zeta potential with a value of 4.1 mV, which suggested to us that the negatively charged functional groups on the GO platelets were covered and stabilized by the positively charged polycations in PIL. From the scanning electron microscopy (SEM) and high-resolution tunneling electron microscopy (TEM) images shown in Figure 1b,c, most of the PIL:RG-O platelets were observed to form separated thin sheets with single- or few-layered structures, which may contribute to the higher effective surface area accessible by the electrolyte ions. X-ray photoelectron spectroscopy (XPS) spectra of the PIL:RG-O material (Supporting Information, Figure S1) showed two N 1s peaks for the imidazolium cation and NTf_2 ($CF_3SO_2-N-SO_2CF_3$) anion, which reflected the coating of PIL on the RG-O platelets, presumably *via* an attractive cation−π interaction. We believe that the PIL intercalated between the overlapped and stacked RG-O platelets improved the wettability with IL-based electrolytes due to the structural similarity of the chosen PIL and IL and thus led to the enhancement of the overall supercapacitor performance.

To evaluate the potential of the thermally reduced PIL:RG-O material for use as an electrode in supercapacitors, a simple two-electrode cell depicted schematically in Figure 1d was used. This device consisted of two PIL:RG-O electrodes on current collectors that were impregnated with the IL electrolyte (EMIM-NTf_2) and a porous propylene separator. The mass of the RG-O (excluding the PIL) coated on each current collector was determined to be 5 mg by thermogravimetric analysis (TGA; Supporting Information Figure S2). The PIL:RG-O electrodes and separator were sandwiched together in a stainless steel cell for the fully assembled two-electrode cell device.

Figure 2a shows cyclic voltammetry (CV) curves obtained from the supercapacitor assembled with PIL:RG-O electrodes and IL electrolytes for voltages up to 3 V with scan rates of 40, 60, and 80 mV/s. The CV curves were close to being rectangular in shape even at the scan rate of 80 mV/s, which is typical capacitive behavior for graphene-based supercapacitors.[6] Although the presence of the functional groups on the surface of the

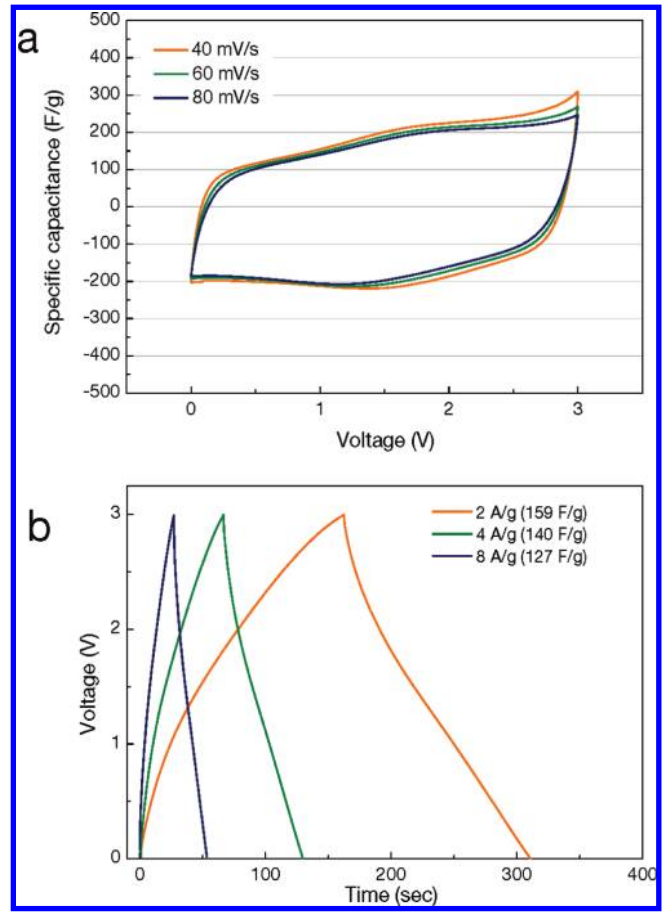

Figure 2. (a) Cyclic voltammogram (CV) at various scan rates for the supercapacitor cell. The test cell was cycled to 3.0 V. (b) Galvanostatic charge/discharge curve at different constant currents. Specific capacitance values are calculated from the discharge curve for each current.

RG-O sheets likely contributed to a small amount of pseudocapacitance, the linearity of the measured current indicates that our devices are primarily nonfaradaic within this voltage window.[6,7] Figure 2b shows a galvanostatic charge/discharge curve at a constant current of 10, 20, and 40 mA (corresponding to a charge/discharge current density of 2, 4, and 8 A/g, respectively), displaying a nearly linear response and thus excellent capacitive behavior. However, a rather slow discharge process was observed at the beginning of each discharge after an appreciable IR drop. The internal resistance value was calculated as 9 Ω from the IR drop, which is slightly higher than that of supercapacitors with aqueous (*e.g.*, aqueous H_2SO_4 or KOH) or organic (*e.g.*, TEA/BF_4 in acetonitrile or propylene carbonate) electrolytes in the absence of PIL modification. A rather slow charge−discharge process and high internal resistance most likely arise from the lower conductivity value of the EMIM-NTf_2 electrolyte (~5 mS/cm) and higher viscosity (28 cP at 20 °C), as compared to aqueous electrolytes.[16] Current work on the design of ILs with high ion conductivity is underway in an effort to address these issues.

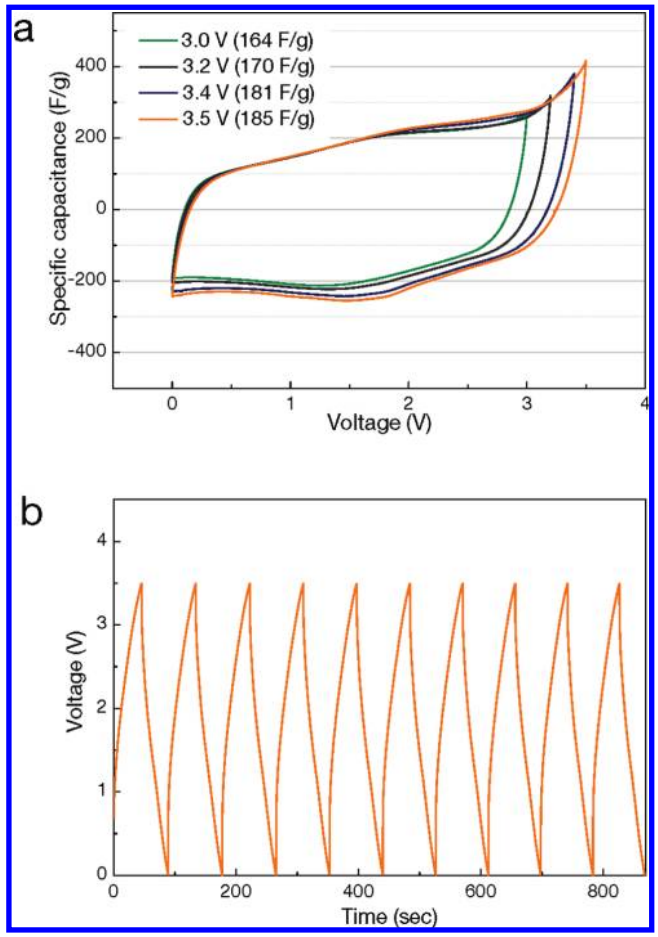

Figure 3. (a) CV curves of the supercapacitor cycled to different maximum voltages (scan rate: 60 mV/s). (b) Galvanostatic charge/discharge curves at a voltage of 3.5 V (current density: 8 A/g).

Nevertheless, the device assembled with PIL:RG-O electrode and IL electrolyte was stable up to 3.5 V, as shown in Figure 3, which is attributed to the superior electrochemical stability of the EMIM-NTf_2 electrolyte, relative to that of the aqueous or organic electrolyte (1 or ~3 V, respectively). This higher operating voltage obtained with our device allows for higher energy densities to be achieved, as discussed below. We note that the CV curves became asymmetric with an increasing pseudocapacitive behavior (Supporting Information Figure S6) when the potential was increased beyond 3.5 V. Hence, a maximum cell voltage up to 3.5 V was used for the evaluation of the device performance.

The specific capacitances (C_{sp}) were calculated from the galvanostatic discharge curves using $C_{sp} = 2 \times I/(-\Delta V/\Delta t)m$, where I is the applied current, $\Delta V/\Delta t$ is the slope of the discharge curve, and m is the mass of RG-O on one electrode. $\Delta V/\Delta t$ was calculated from the upper half of the discharge curve after the IR drop, that is, $\Delta V/\Delta t = (V_{max} - 1/2V_{max})/(T_2 - T_1)$, since the apparent capacitance values can be inflated by including the lower half of the discharge curve.[17] Figure 4a presents the specific capacitance plotted *versus* the current density at different operating voltages, in which the maximum value reached 187 F/g at 3.0 V and saturated at 127 F/g with increasing current density. The specific capacitance values ranging from 127 to 187 F/g are significantly higher than the values obtained with carbon nanotube (CNT) or graphene-based supercapacitors using aqueous or organic electrolytes.[6,15,18,19] We also note that the control supercapacitor cell with RG-O electrodes that were not modified with PIL showed specific capacitance values in the range from 115 to 132 F/g (Supporting Information Figure S5), which were significantly lower than for the cell with PIL:RG-O electrodes. Given the high specific capacitance values with our device, we surmise that the wetting of the electrodes with IL electrolyte was facilitated by the functional PIL molecules on the RG-O surface, which then increased the effective surface area accessible by electrolyte ions. Indeed, the IL electrolyte employed (*i.e.*, EMIM-NTf_2) is hydrophobic in nature mainly due to the fluorine-containing anions (NTf_2^-)[10,20] and is, therefore, expected to exhibit high affinity toward hydrophobic electrode materials. On the other hand, chemically or thermally reduced graphene oxide (RG-O) is at least partially hydrophilic because there is a significant amount of oxygen-containing functional groups (such as epoxide, hydroxyl, and carboxylic groups) present on their basal plane and at the edges,[21,22] which might also act as the active sites for redox reactions. Hence, the compatibility between the EMIM-NTf_2 and the RG-O electrode may be diminished unless the surface of the RG-O platelets is modified. In the case of PIL:RG-O electrodes, hydrophilic groups present on RG-O plates are mostly covered by the PIL molecules bearing the hydrophobic NTf_2 anion, which in turn leads to the electrode surface being more hydrophobic and more compatible with EMIM-NTf_2, as shown by contact angle measurements (Supporting Information Figure S3).

In addition, the ion sizes of the IL electrolyte are estimated to be 0.79 and 0.76 nm in the longest dimension for EMIM cation and NTf_2 anion, respectively.[13] The RG-O platelets are known to have an interlayer spacing much less than 0.8 nm,[15,23] which might be too small for the effective accessibility of IL electrolyte, re-emphasizing the role of surface modification of graphene materials in their application in high-performance supercapacitors. Moreover, X-ray diffraction (XRD) pattern of PIL:RG-O samples (Supporting Information Figure S4) showed no dominant peak that is normally observed for G-O and RG-O platelets. This result suggested to us that a highly disordered overlay of individual RG-O platelets formed in the PIL matrix, which may provide an interlayer spacing accessible to the ions of IL electrolytes.

To investigate whether surface modification with PIL can be extended into other types of carbon electrodes, comparative experiments with the same PIL were applied to activated carbons (ACs) without RG-O platelets present. The CV curves of the PIL-modified AC

electrodes (Supporting Information Figure S8) showed specific capacitance values of 28 F/g. This result is consistent with the PIL is blocking the pores of the ACs to such an extent that the IL electrolyte cannot penetrate. For example, the PIL-modified AC electrodes exhibited far lower specific areas as measured using the Brunauer−Emmett−Teller (BET) method (values shown in Supporting Information Table S2). Given the apparent blocking of mesopores by the PIL, it would seem that good options for electrode materials include those having relatively high aspect ratios such as conductive platelets and conductive nanorods. For example, it is reasonably likely that a good configuration for SWNTs can be found where they would be PIL-coated and combined with an appropriate IL. Other options could include 3D solids with significantly larger pore size distributions than are present in the typical activated carbon currently used in supercapacitors; of course, this may lead to situations where the specific surface area accessible to the electrolyte is not high enough. Further work in these directions is underway.

On the basis of the above results, the power (P) and energy (E) densities of our supercapacitors were calculated using $P = V^2/4RM$ and $E = 0.5 \times CV^2/M$,[24] where V is the voltage applied, M is the total mass of the PIL:RG-O electrodes, C the measured device capacitance, and R the equivalent series resistance determined from the IR drop in the galvanostatic discharge curve. The corresponding energy density *versus* power density is shown with the operating voltages in Figure 4b. The energy and power density values are normalized both to the total mass of two electrodes including all components such as the electrodes, electrolyte, and current collectors and to the mass of two electrodes not including the mass of electrolyte. The maximum energy density of our device obtained at an operating voltage of 3.5 V was 6.5 W · h/kg, which is comparable to or higher than the values previously reported,[25] and the maximum power density was 2.4 kW/kg. As discussed earlier, the use of EMIM-NTf_2 takes advantage of its larger electrochemical stability window, allowing for operation at 3.5 V, which in turn increased both the energy density and power density of the device.

To further evaluate the device performance, the frequency response of the supercapacitor incorporating the PIL:RG-O electrodes and EMIM-Tf_2N electrolyte was analyzed using electrical impedance spectroscopy (EIS). Figure 5 shows the Nyquist plot in the frequency range of 0.05 Hz to 1 MHz, with the lower left portion of the curve corresponding to the higher frequency. The depressed semicircle in the high-frequency region is modeled by a parallel combination of an interfacial charge transfer resistance and the double-layer capacitance.[1,26] The inclined portion of the curve spanning real resistances (Z') of approximately 3.0 to 6.0 Ω is typically represented by the Warburg impedance that pertains to

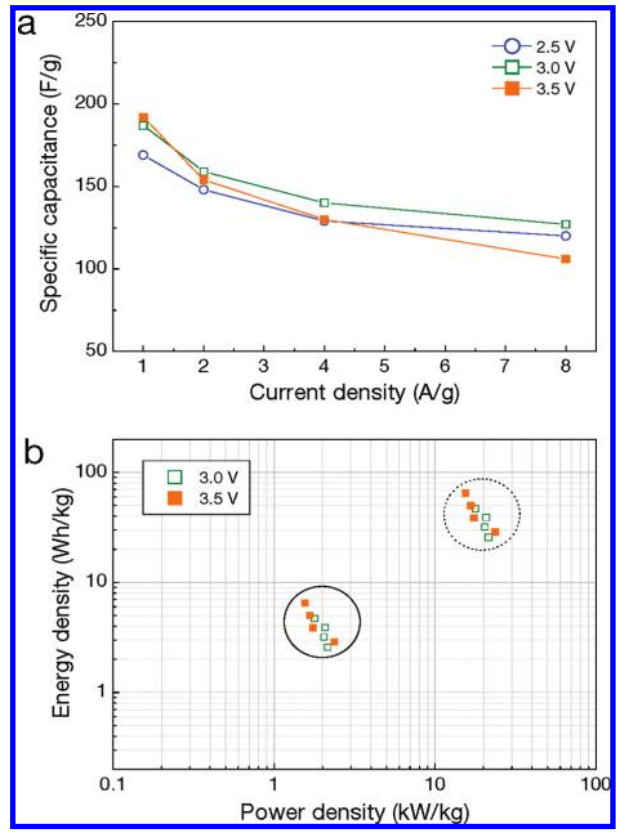

Figure 4. (a) Plot of specific capacitance *versus* the current density. The specific capacitance value was obtained from the galvanostatic charge/discharge measurement. (b) Plot of energy density *versus* power density at operating voltages of 3.0 and 3.5 V. The energy and power density were normalized to the total mass of the two electrodes employed including the electrolyte and current collector (solid circle) and the mass of two PIL:RG-O (dashed circle).

ion diffusion and transport in the electrolyte.[1,6] A short Warburg region on the plot can be explained by increased ion diffusion within the PIL:RG-O electrodes due to the enhanced compatibility between the electrode and IL electrolyte. The excellent capacitive behav-

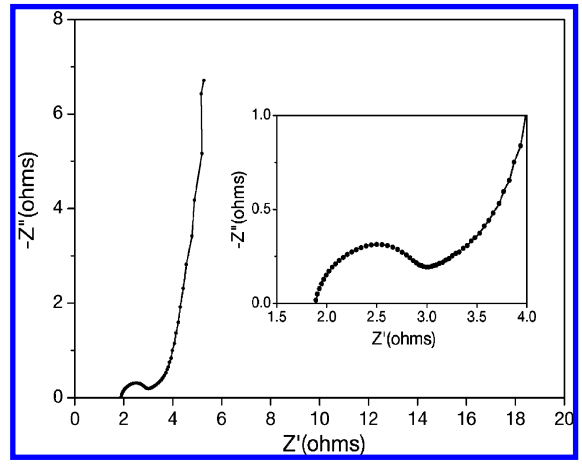

Figure 5. Nyquist plot (a plot of the imaginary component, Z'' *versus* the real component, Z' of the impedance) for the supercapacitor incorporating a PIL:RG-O electrode over the frequency range from 0.05 to 1 M Hz. The inset shows the enlarged high-frequency region of the plot.

ior of our supercapacitor is also confirmed by a nearly vertical line at low frequencies. From the extrapolation of the vertical portion of the Nyquist plot to the real axis, the equivalent series resistance (ESR) was estimated to be 3.7 Ω for our device, which is higher than the values of classical electrolytes.[6] As previously mentioned, this is likely due to the lower electrical conductivity and higher viscosity of EMIM-NTf_2, relative to aqueous electrolytes. Nevertheless, the negative impact from the lower ionic conductivity of the IL electrolyte may be offset by the increase in the operating voltage for achieving high energy and power density.

In conclusion, the present work demonstrates that the general concept of a supercapacitor design based on PIL-modified reduced graphene oxide electrodes and a compatible IL electrolyte holds potential as an electrical energy storage device. Poly(1-vinyl-3-ethylimidazolium) salts bearing the bis(trifluoromethylsulfonyl)amide anion (NTf_2^- or $CF_3SO_2-N-SO_2CF_3$) as the PIL and EMIM-NTf_2 as the IL electrolyte were studied. Cyclic voltammetry and galvanostatic charge−discharge results indicate stable electrochemical performance, and a specific capacitance as high as 187 F/g was measured and found to be reproducible (Supporting Information, Table S1). This relatively high capacitance is presumably due to improved wettability of the chosen IL electrolyte on the PIL-modified reduced graphene oxide materials which, synergistically, enhanced the effective surface area of the electrode/electrolyte interfaces. A maximum energy density of 6.5 W · h/kg with a maximum power density of 2.4 kW/kg was also observed. Even though further work is needed to optimize the device for faster charge−discharge response, our current approach may provide a promising technique for the fabrication of high-performance supercapacitors.

METHODS

PIL-Modified Reduced Graphene Oxide (PIL:RG-O) Materials. Graphite oxide (GO) was synthesized from natural flake graphite (Bay Carbon, SP-1) using a modified Hummers method.[27] PIL of poly(1-vinyl-3-ethylimidazolium) bis(trifluoromethylsulfonyl)amide with an average molecular weight (M_w) of 170 kDa was synthesized according to a previously reported procedure.[28,29] First, 75 mg of PIL was completely dissolved in 20 mL of anhydrous propylene carbonate (PC) by stirring for 30 min at room temperature. Then, 20 mg of GO powder was suspended *via* mild sonication in the PC solution containing PIL. In a typical process, a uniform brown-colored suspension of graphene oxide (G-O) with PIL in PC solvent with a concentration of 1.0 mg/mL was obtained by 1 h of sonication. Zeta potential measurements (ELSZ-2, Otsuka electronics) were performed on the G-O suspension in PC and PIL-modified G-O suspension in PC. Thermal reduction of G-O platelets was carried out in an oil bath by heating the suspension at 150 °C,[15] which yielded a homogeneous black-colored suspension of PIL-modified reduced graphene oxide (PIL:RG-O) in PC within an hour. SEM images of the PIL-G samples were obtained with a field emission scanning electron microscope (Hitachi S-4300). TEM images were taken with TECNAI 20 microscope by placing a few drops of PIL:RG-O suspension on a copper grid and followed by evaporation in a vacuum oven.

Fabrication of Supercapacitors Based on PIL:RG-O Electrodes. The PIL:RG-O was collected on a Teflon membrane (0.2 μm pore size) by vacuum filtration. Then, PIL:RG-O materials were impregnated with a drop of IL electrolyte, 1-ethyl-3-methylimidazolium bis(trifluoromethylsulfonyl)amide (EMIM-NTf_2) (Basionics HP01, BASF) under filtration, and used as the electrode without any additional binder or additives. The electrodes were formed from a thick slurry and pressed onto the carbon-coated Al current collector. Each electrode had a diameter of 20 mm and a thickness of approximately 100 μm. The PIL:RG-O electrodes and a porous polypropylene separator (Celgard 3501) were sandwiched together in a stainless steel cell for the fully assembled two-electrode cell device. Electrochemical data were obtained using cyclic voltammetry, chronopotentiometry, and electrical impedance spectroscopy (EIS) (Solartron analytical 1400/1470E celltest system).

Acknowledgment. T.Y.K., H.W.L., and K.S.S. were supported by InsCon Tech, Co. Ltd., South Korea. M.S., D.R.D., C.W.B., and R.S.R. were supported by the U.S. DoE under Award DE-ER46657.

Supporting Information Available: Additional characterization (XPS, XRD, and TGA) and supercapacitor testing data. This material is available free of charge *via* the Internet at http://pubs.acs.org.

REFERENCES AND NOTES

1. Conway, B. E. *Electrochemical Supercapacitors: Scientific Fundamentals and Technological Applications*; Kluwer Academics and Plenum: New York, 1999.
2. Simon, P.; Gogotsi, Y. Materials for Electrochemical Capacitors. *Nat. Mater.* **2008**, *7*, 845–854.
3. Miller, J. R.; Simon, P. Electrochemical Capacitors for Energy Management. *Science* **2008**, *321*, 651–652.
4. Geim, A. K.; Novoselov, K. S. The Rise of Graphene. *Nat. Mater.* **2007**, *6*, 183–191.
5. Novoselov, K. S.; Geim, A. K.; Morozov, S. V.; Jiang, D.; Zhang, Y.; Dubonos, S. V.; Grigorieva, I. V.; Firsov, A. A. Electric Field Effect in Atomically Thin Carbon Films. *Science* **2004**, *306*, 666–669.
6. Stoller, M. D.; Park, S.; Zhu, Y.; An, J.; Ruoff, R. S. Graphene-Based Ultracapacitors. *Nano Lett.* **2008**, *8*, 3498–3502.
7. Wang, Y.; Shi, Z.; Huang, Y.; Ma, Y.; Wang, C.; Chen, M.; Chen, Y. Supercapacitor Devices Based on Graphene Materials. *J. Phys. Chem. C* **2009**, *113*, 13103–13107.
8. Stankovich, S.; Dikin, D. A.; Dommett, G. H. B.; Kohlhaas, K. M.; Zimney, E. J.; Stach, E. A.; Piner, R. D.; Nguyen, S. T.; Ruoff, R. D. Graphene-Based Composite Materials. *Nature* **2006**, *442*, 282–286.
9. Kötz, R.; Carlen, M. Principles and Applications of Electrochemical Capacitors. *Electrochim. Acta* **2000**, *45*, 2483–2498.
10. Armand, M.; Endres, F.; MacFarlane, D. R.; Ohno, H.; Scrosati, B. Ionic-Liquid Materials for the Electrochemical Challenges of the Future. *Nat. Mater.* **2009**, *8*, 621–629.
11. Sato, T.; Masuda, G.; Takagi, K. Electrochemical Properties of Novel Ionic Liquids for Electric Double Layer Capacitor Applications. *Electrochim. Acta* **2004**, *49*, 3603–3611.
12. Tasuda, T.; Hussey, C. L. Electrochemical Applications of Room-Temperature Ionic Liquids. *Electrochem. Soc. Interface* **2007**, *16*, 42–49.
13. Largeot, C.; Portet, C.; Chmiola, J.; Taberna, P.; Gogotsi, Y.; Simon, P. Relation between the Ion Size and Pore Size for an Electric Double-Layer Capacitor. *J. Am. Chem. Soc.* **2008**, *130*, 2730–2731.
14. Kim, T.; Lee, H.; Kim, J.; Suh, K. S. Synthesis of Phase Transferable Graphene Sheets Using Ionic Liquid Polymers. *ACS Nano* **2010**, *4*, 1612–1618.

15. Zhu, Y.; Stoller, M. D.; Cai, W.; Velamakanni, A.; Piner, R. D.; Chen, D.; Ruoff, R. S. Exfoliation of Graphene Oxide in Propylene Carbonate and Thermal Reduction of the Resulting Graphene Oxide Platelets. *ACS Nano* **2010**, *4*, 1227–1233.
16. Lu, W.; Henry, K.; Turchi, C.; Pellegrino, J. Incorporating Ionic Liquid Electrolytes into Polymer Gels for Solid-State Ultracapacitors. *J. Electrochem. Soc.* **2008**, *155*, A361–A367.
17. Stoller, M. D.; Ruoff, R. S. Methods and Best Practices for Determining an Electrode Material's Performance for Ultracapacitors. *Energy Environ.* **2010**, *3*, 1294–1301.
18. Niu, C.; Sichel, E. K.; Hoch, R.; Moy, D.; Tennent, H. High Power Electrochemical Capacitors Based on Carbon Nanotube Electrodes. *Appl. Phys. Lett.* **1997**, *70*, 1480–1482.
19. An, K. H.; Kim, W. S.; Park, Y. S.; Moon, J. M.; Bae, D. J.; Lim, S. C.; Lee, Y. S.; Lee, Y. H. Electrochemical Properties of High Power Supercapacitors Using Single-Walled Carbon Nanotube Electrodes. *Adv. Funct. Mater.* **2001**, *11*, 387–392.
20. Wang, X.; Fulvio, P. F.; Baker, G. A.; Veith, G. M.; Unocic, R. R.; Mahurin, S. M.; Chi, M.; Dai, S. Direct Exfoliation of Natural Graphite into Micrometer Size Few Layers Graphene Sheets Using Ionic Liquids. *Chem. Commun.* **2010**, *46*, 4487–4489.
21. Stankovich, S.; Dikin, D. A.; Piner, R. D.; Kohlhaas, K. A.; Kleinhammes, A.; Jia, Y.; Wu, Y.; Nguyen, S. T.; Ruoff, R. S. Synthesis of Graphene-Based Nanosheets *via* Chemical Reduction of Exfoliated Graphite Oxide. *Carbon* **2007**, *45*, 1558–1565.
22. Park, S.; An, J.; Piner, R. D.; Jung, I.; Yang, D.; Velamakanni, A.; Nguyen, S. T.; Ruoff, R. S. Aqueous Suspension and Characterization of Chemically Modified Graphene Sheets. *Chem. Mater.* **2008**, *20*, 6592–6594.
23. Park, S.; An, J.; Jung, I.; Piner, R. D.; An, S. J.; Li, X.; Velamakanni, A.; Ruoff, R. S. Colloidal Suspensions of Highly Reduced Graphene Oxide in a Wide Variety of Organic Solvents. *Nano Lett.* **2009**, *9*, 1593–1597.
24. Frackowiak, E. Carbon Materials for Supercapacitor Application. *Phys. Chem. Chem. Phys.* **2007**, *9*, 1774–1785.
25. Kaempgen, M.; Chan, C. K.; Ma, J.; Cui, Y.; Gruner, G. Printable Thin Film Supercapacitors Using Single-Walled Carbon Nanotubes. *Nano Lett.* **2009**, *9*, 1872–1876.
26. Randles, J. E. B. Kinetics of Rapid Electrode Reactions. *Discuss. Faraday Soc.* **1947**, *1*, 11–19.
27. Hummers, W. S.; Offerman, R. E. Preparation of Graphitic Oxide. *J. Am. Chem. Soc.* **1958**, *80*, 1339.
28. Kim, T. Y.; Lee, T. H.; Kim, J. E.; Kasi, R. M.; Sung, C. S. P.; Suh, K. S. Organic Solvent Dispersion of Poly(3,4-ethylenedioxythiophene) with the Use of Polymeric Ionic Liquid. *J. Polym. Sci., Polym. Chem.* **2008**, *46*, 6872–6879.
29. Marcilla, R.; Ochioteco, E.; Pozo-Gonzalo, C.; Grande, H.; Pomposo, J. A.; Mecerreyes, D. New Organic Dispersions of Conducting Polymers Using Polymeric Ionic Liquids as Stabilizers. *Macromol. Rapid Commun.* **2005**, *26*, 1122–1126.